Pharm Res (2014) 31:2404–2419
DOI 10.1007/s11095-014-1336-0

RESEARCH PAPER

In Vitro and *In Situ* Evaluation of pH-Dependence of Atazanavir Intestinal Permeability and Interactions with Acid-Reducing Agents

Olena Kis • Sharon L. Walmsley • Reina Bendayan

Received: 20 November 2013 / Accepted: 8 February 2014 / Published online: 5 March 2014

ABSTRACT

Purpose The objectives of this study were to evaluate the effects of intestinal lumen pH, food intake, and acid-reducing agents on the intestinal permeability of atazanavir, an HIV-1 protease inhibitor.

Methods Atazanavir permeability across Caco-2 cell monolayers (P_{app}) and *in situ* steady-state permeability across rat jejunum and ileum (P_{eff}) were evaluated in buffers of varied pH (4.5–8.5), in fasted- or fed-state simulated intestinal fluid, or in presence of acid-reducing drugs (*e.g.*, omeprazole).

Results *In vitro* accumulation and apical-to-basolateral P_{app} of atazanavir increased with decreasing pH. This effect appeared to be associated with lower atazanavir efflux by P-glycoprotein at acidic pH (5.5) compared to neutral pH. *In situ* atazanavir P_{eff} across rat jejunum and ileum also decreased 2.7 and 2.3-fold, respectively, when pH was increased from 4.5 to 8.5. Several acid-reducing agents (*e.g.*, omeprazole) moderately inhibited atazanavir efflux in Caco-2 monolayers; however, this effect was not observed *in situ*. Fed-state buffer significantly increased atazanavir apical-to-basolateral P_{app} ($p < 0.001$) and *in situ* P_{eff} ($p < 0.05$) compared to fasted-state buffer.

Conclusions Atazanavir permeability is sensitive to changes in intestinal lumen pH. This pH-sensitivity may contribute to atazanavir clinical interactions with acid-reducing agents and variable oral bioavailability.

O. Kis • R. Bendayan (✉)
Department of Pharmaceutical Sciences, Leslie Dan Faculty of Pharmacy
University of Toronto, 144 College Street, Room 1001
Toronto, Ontario M5S 3M2, Canada
e-mail: r.bendayan@utoronto.ca

S. L. Walmsley
Department of Medicine University of Toronto
Toronto, Ontario Canada

S. L. Walmsley
Division of Infectious Diseases University Health Network
Toronto, Ontario Canada

KEY WORDS acid-reducing agents · atazanavir · HIV-1 protease inhibitors · intestinal permeability · pH dependence

ABBREVIATIONS

AUC	area under the curve
C_{max}	maximum or peak plasma concentration
CYP	cytochrome P450
H_2RA	histamine$_2$-receptor antagonist
HIV	human immunodeficiency virus
MRP	multidrug resistance-associated protein
OATP	organic anion transporting polypeptide
Pgp	P-glycoprotein
PPI	proton-pump inhibitor
SIF	simulated intestinal fluid

INTRODUCTION

Atazanavir is an HIV-1 protease inhibitor used in combination with other antiretroviral drugs for clinical management of HIV infection (1). Although atazanavir clinical use is generally well tolerated, high interindividual variability in atazanavir pharmacokinetics and many clinically significant drug-drug interactions can compromise its efficacy and safety (2). Oral administration of 400 mg/day atazanavir in HIV-infected patients results in a maximum (peak) plasma concentration (C_{max}) of 3.15±2.23 μg/ml and area under the curve (AUC) of 22.3±20.2 μg•h/ml (3). In contrast, healthy individuals have higher and less variable C_{max} (5.36±1.37 μg/ml) and AUC (29.3±8.3 μg•h/ml) (2). Although the reasons for these pharmacokinetic differences remain unclear, atazanavir exhibits pH-dependent aqueous solubility, which decreases when pH is increased above 3 (2,4), and HIV-infected patients are reported to have increased gastric pH due to common gastrointestinal complications associated with HIV infection (5). In addition, atazanavir bioavailability is affected by food

intake. Relative to fasting levels, atazanavir administration with a light meal increases its AUC and C_{max} by 70% and 57%, respectively, for unboosted atazanavir regimens, and 33% and 40%, respectively, for ritonavir-boosted regimens (2). Since food intake is associated with the secretion of acid in the stomach and bile salts (*e.g.*, taurocholate) and phospholipids (*e.g.*, lecithin) in the small intestine, observed enhancement in atazanavir oral bioavailability may be related to the changes in atazanavir intestinal permeability mediated by pH or composition of the intestinal fluid.

Clinical use of atazanavir is associated with many drug-drug interactions involving acid-reducing agents, such as proton-pump inhibitors (PPIs), histamine$_2$-receptor antagonists (H_2RAs), and antacids (3,6–8). Since these drugs increase gastrointestinal pH, these interactions are suggested to be pH-mediated. However, depending on the acid-reducing agent used, the magnitude of the effect on atazanavir pharmacokinetics differs considerably. Studies in healthy volunteers receiving ritonavir-boosted atazanavir demonstrated that co-administration of 40 mg of omeprazole (PPI) decreased atazanavir AUC, C_{max}, and minimum (trough) plasma concentration by 72%, 76%, and 78%, respectively (8), while 40 mg of famotidine (H_2RA) reduced atazanavir AUC and C_{max} only by 20–25% (9). Although one potential explanation for these differences is that omeprazole has a more potent effect on gastric pH (10), other mechanisms independent of the effect of acid-reducing agents on gastric pH may contribute to these clinical drug-drug interactions.

Atazanavir is a bulky azapeptide drug (free base molecular weight of 704.9) with poor aqueous solubility (3.27×10^{-3} g/l) and high lipophilicity (predicted log *P* value of 4.08–4.54) (http://www.drugbank.ca/drugs/DB01072) (2). However, experimentally it was shown to have lower octanol:saline partition coefficient of 29.90 ± 4.12 equivalent to log P of 1.48 (11). Atazanavir contains a weakly basic ionisable group with predicted pKa of 4.4. While at neutral pH it is primarily uncharged, at acidic pH, the basic group becomes protonated and positively charged, increasing atazanavir aqueous solubility. Based on the predicted high permeability (log *P* value > 1.72) and low aqueous solubility, atazanavir can be classified as a Class 2 compound in the Biopharmaceutics Classification System (BCS), with the predicted absorption of ≥90% (12). Atazanavir is also highly metabolized (approximately 80% of 400-mg oral dose) primarily by cytochrome P450 (CYP) enzymes (*i.e.*, CYP3A4) (2). In addition, atazanavir is a substrate for membrane-associated drug transporters, such as P-glycoprotein (Pgp) and multidrug resistance-associated proteins (MRPs), and an unidentified uptake carrier potentially belonging to the organic anion transporting polypeptide (OATP) superfamily (11,13–15). Many PPIs are known to interact with metabolic enzymes and drug transporters (10). For example, omeprazole competitively inhibits CYP3A4 and CYP2C19, induces the activity of CYP3A4, CYP2C19, and CYP1A2, and inhibits efflux transporters, Pgp and breast cancer resistance protein (16). Similarly, H_2RAs are known to interact with several drug uptake and efflux transporters. Cimetidine can competitively inhibit organic cation transporters 1 and 2 as well as organic cation efflux transporters, such as multidrug and toxin extrusion transporters 1 and 2-K (17). Hence, potential pharmacokinetic interactions of these drugs with atazanavir transport or metabolism could contribute to the observed clinical drug-drug interactions. To the best of our knowledge, no studies evaluating the effects of PPIs or H_2RAs on atazanavir intestinal permeability or demonstrating that atazanavir intestinal permeability is altered by changes in pH are available. In this study, we used an established *in vitro* human epithelial cell line system (Caco-2) and an *in situ* intestinal perfusion model to investigate atazanavir intestinal permeability at various intestinal luminal pH or fasted- or fed-state conditions and assess potential pharmacokinetic interactions with coadministered acid-reducing agents.

MATERIALS AND METHODS

Materials

^{3}H-Atazanavir (3 Ci/mmol) and ^{14}C-D-mannitol (55 mCi/mmol) were purchased from Moravek Biochemicals (Brea, CA). Valspodar, *i.e.*, PSC833 (chemical name: 6-[(2S,4R,6E)-4-methyl-2-(methylamino)-3-oxo-6-octenoic acid]-7-L-valine-cyclosporin A), was a generous gift from Novartis Pharma (Basel, Switzerland). Unlabeled atazanavir was obtained from the National Institutes of Health AIDS research and reference reagent program, Division of AIDS, National Institute of Allergy and Infectious Diseases, National Institutes of Health (Bethesda, MD). Caco-2 cells were obtained from the American Type Culture Collection (Manassas, VA). Tissue culture reagents such as Dulbecco's Modified Eagle's Medium, L-glutamine, penicillin/streptomycin, minimal essential medium non-essential amino acids, fetal bovine serum, phosphate-buffered saline (PBS), and trypsin were obtained from Invitrogen (Grand Island, NY, USA). Drugs (PPIs and H_2RAs), sodium taurocholate, egg lecithin (L-α-phosphatidylcholine), all biological buffers, Triton X-100, and all other reagents were purchased from Sigma-Aldrich (Oakville, Canada), unless otherwise indicated.

Preparation of Buffers for *In Vitro*, *In Situ*, and Lipophilicity Experiments

For *in vitro* transport assays and *in situ* perfusion studies, buffers of varied pH (4.5–8.5) were prepared using 135 mM NaCl and 5 mM KCl stock solution supplemented with 25 mM

acetic acid for pH 4.5 buffer, 25 mM MES [chemical name: 2-(N-morpholino)ethanesulfonic acid] for pH 5.5 buffer, 25 mM BES [chemical name: N,N-Bis(2-hydroxyethyl)-2-aminoethanesulfonic acid] for pH 6.5 buffer, 25 mM HEPES [chemical name: 4-(2-hydroxyethyl)-1-piperazineethanesulfonic acid] for pH 7.4 buffer, or 25 mM Tris buffer [chemical name: 2-amino-2-(hydroxymethyl)propane-1,3-diol] for pH 8.5 buffer. For Transwell permeability studies, basolateral compartment and preincubation buffers were prepared using Hanks' balanced salt solution (1.3 mM $CaCl_2$, 0.49 mM $MgCl_2$, 0.41 mM $MgSO_4$, 5.3 mM KCl, 0.44 mM KH_2PO_4, 138 mM NaCl, 0.34 mM Na_2HPO_4, and 5.6 mM D-glucose), supplemented with 25 mM HEPES. Each buffer was adjusted to the desired pH by addition of 1 N HCl or 1 N NaOH solution and pH was measured using VWR SympHony Model SB70P pH meter (VWR, Mississauga, Canada). For *in vitro* accumulation and permeability experiments, all buffers were supplemented with 0.01% bovine serum albumin (BSA) to reduce the binding of radiolabeled compounds to glass and plastic surfaces. For experiments examining atazanavir lipophilicity, same pH 4.5–8.5 buffers were used as described above for *in vitro* transport studies, but without 0.01% BSA. In addition, buffers of pH 1, 2, 3, and 4 were prepared using 50 mM KCl solution (for pH 1 and 2) and 50 mM potassium hydrogen phthalate (for pH 3 and 4) (18).

Solutions simulating intestinal fluid in the fed or fasted state were prepared as described previously (19). Briefly, to prepare fasted-state simulated intestinal fluid (SIF), 6.2 g/l of NaCl and 3.4 g/l of NaH_2PO_4 were dissolved in deionized water and the pH of the solution was adjusted to pH 6.5 using 1 N NaOH. This "blank" fasted-state SIF buffer was then supplemented with 3 mM sodium taurocholate and 0.75 mM egg lecithin. To prepare fed-state SIF buffer, 11.9 g/l of NaCl and 8.65 g/l of CH_3COOH were dissolved in deionized water and the pH of the solution was adjusted to pH 5.0 using 1 N NaOH. This "blank" fed-state SIF buffer was supplemented with 15 mM sodium taurocholate and 3.75 mM egg lecithin. Taurocholate and lecithin were stirred into the fasted- and fed-state SIF overnight using a magnetic stir plate until a clear micellar solution was formed.

Determination of Atazanavir Lipophilicity at Different pH

Lipophilicity of atazanavir across a range of pH (1–8.5) was determined using 1:1 mixture of 1-octanol or cyclohexane and the aqueous buffer of varied pH (*i.e.*, water layer). The selection of the two organic solvents was based on their differences in hydrogen bonding capacity. While 1-octanol allows hydrogen bonding, cyclohexane does not. Prior to mixing organic and aqueous phases, ^{3}H-labeled atazanavir (0.2 μCi/ml) solution, supplemented with unlabeled drug to a final concentration of 10 μM, was prepared in buffers of different pH (1–8.5). At 10 μM concentration, atazanavir was fully dissolved in the aqueous solution across this range of pH values. Samples of each solution were taken to measure the radioactivity corresponding to the total 10 μM atazanavir (*i.e.*, 100%). Equal volumes of each aqueous solution (containing ^{3}H-atazanavir) and organic solvent (1-octanol or cyclohexane) were combined and shaken repeatedly over 30 min period and allowed to equilibrate for at least 24 h. Mixtures were then centrifuged at 800×g for 30 min at 22°C and atazanavir concentration remaining in the aqueous layer was determined by liquid scintillation counting. Log D values were estimated from the apparent partitioning coefficients ($D = C_{organic}/C_{aqueous}$) determined at each pH, where $C_{aqueous}$ is the concentration of atazanavir in the aqueous solvent and $C_{organic}$ is the concentration of atazanavir in the organic solvent (estimated by deducting atazanavir remaining in the aqueous compartment after mixing from the total amount measured initially prior to mixing with the organic solvent). Log D coefficients describe the pH dependent partitioning of both ionized and unionized forms of the compound between the organic and aqueous solutions, whereas log P coefficients refer to the partition coefficients determined in the octanol:water mixture or the calculated partition coefficients, which are independent of pH.

Cell Culture

Caco-2 cells were maintained at 37°C and 5% CO_2 in cell culture medium consisting of Dulbecco's Modified Eagle's Medium (4.5 g/L glucose), 10% fetal bovine serum, 2 mM L-glutamine, 1% minimal essential medium non-essential amino acids, and 1% penicillin/streptomycin. Cells were passaged using 0.05% trypsin-EDTA upon reaching 95% confluence. For atazanavir transport studies, Caco-2 cells (passage number 40–55) were seeded at 6×10^4 cells/cm^2 cell density on the surface of flat-bottom 48-well plates (for intracellular accumulation assays) or 12-well, 0.4 μm pore size Transwell™ polycarbonate membrane inserts (for permeability assays). Culture medium was replaced 24 h after passaging and every 2–3 days thereafter for 20–22 days post-confluence to achieve small intestine-like epithelial cell differentiation (20).

Transport Experiments in Caco-2 Cells

Atazanavir accumulation assays in Caco-2 cells grown on solid support were performed according to our previous published protocol (21). Briefly, once confluent Caco-2 cell monolayers were fully differentiated (after 20–22 days in culture post-confluence), 48-well plates were placed on a dry bath at 37°C for the duration of the experiment and culture medium in each well was replaced with blank pH 7.4 transport buffer (*i.e.*, preincubation buffer). Cells were allowed to equilibrate for 20 min and the preincubation buffer was replaced by

radioactive transport buffer of desired pH (4.5–8.5) containing 0.1 μCi/ml ^{3}H-atazanavir supplemented with unlabeled atazanavir to reach 1 μM concentration. At the desired time interval, the radioactive buffer was removed and cells were washed twice with ice-cold PBS and solubilised in 1% Triton X-100 at 37°C for 30 min. The content of each well was collected into 7 ml vial, mixed with 2 ml of PicoFluor 40 scintillation fluid (PerkinElmer, Boston, MA), and incubated for 10 min at room temperature. The total radioactivity in each vial was measured using a Beckman Coulter LS6500 Scintillation counter. All accumulation values were corrected using "zero-time" uptake, which was determined in each experiment by measuring the amount of radiolabeled atazanavir retained by the cells after a minimum exposure, *i.e.*, when radioactive solution was removed immediately after it was added into the well. Uptake of the ^{3}H-atazanavir was normalized to the total cellular protein content per well, which was measured in each experiment (average from 3 wells) using the BioRad DC Protein Assay kit (Bio-Rad, Mississauga, Ontario, Canada) and BSA as the standard. To evaluate inhibitory potencies of selected inhibitor drugs, cellular accumulation of ^{3}H-atazanavir was evaluated in the absence (control) or presence of each drug (at specified concentration), which was added to the preincubation buffer and the radioactive transport buffer. For inhibitors dissolved initially in dimethyl sulfoxide (DMSO), equal volume of DMSO was added to the corresponding "control" solution. To evaluate the concentration-dependent effect, cellular accumulation of ^{3}H-atazanavir, after 60 min incubation at pH 7.4, was evaluated in the absence (DMSO control) or presence of different concentrations of omeprazole (0.01–500 μM) or cimetidine (0.01–500 μM). Omeprazole interactions were also evaluated in the presence of 1 μM PSC833, a non-immunosuppressive analog of cyclosporine A and potent inhibitor of Pgp, which was added to the control transport buffer and all omeprazole containing solutions (0.01–500 μM). ^{3}H-Atazanavir accumulation in the presence of various concentrations of omeprazole was expressed as % of control, *i.e.*,^{3}H-atazanavir accumulation in the presence of 1 μM PSC833 without omeprazole added. The concentrations of inhibitor drugs that resulted in half-maximal inhibitory effect (*i.e.*, IC_{50}) were estimated by fitting the data to a sigmoidal dose response equation (Eq. 1).

Atazanavir permeability across Caco-2 cell monolayers was examined by the Transwell drug permeability assay, modified from our method described previously (13). Caco-2 cells, grown on Transwell membrane inserts for 20–22 days post confluence, were washed with PBS at 37°C. The monolayer integrity in each well was confirmed by measuring the transepithelial electrical resistance across the monolayer (> 600 $\Omega \cdot cm^2$ used for experiments) using a Millicell-ERS (Millipore). Each well was transferred into a clean 12-well plate, which was placed on a dry bath at 37°C for the duration of the experiment. Basolateral compartment of each well was filled with 1.5 ml of basolateral buffer and PBS in the apical compartment was replaced with the apical preincubation buffer of pH 7.4 and allowed to equilibrate for 20 min. For measuring apical-to-basolateral permeability at different apical pH, the buffer in the basolateral (receiver) compartment was replaced with 1.5 ml of fresh basolateral buffer (pH 7.4) and the buffer in the apical (donor) compartment was replaced with 0.5 ml of radioactive solution of pH 4.5–8.5 containing 1 μM ^{3}H-atazanavir and 1 μM ^{14}C-D-mannitol. Permeability of ^{14}C-D-Mannitol was used as a control, to confirm monolayer integrity for the length of the flux experiment. To maintain sink conditions, every 15 min (at t= 15 min, 30 min, 45 min, and 60 min) each Transwell was moved into a new well containing fresh basolateral buffer. Atazanavir and D-mannitol concentrations in the basolateral compartment after each time point were then measured by taking two 250 μl samples from each well, combining each one with 2 ml of scintillation fluid and counting ^{3}H and ^{14}C radioactivity by liquid scintillation counting. For measuring basolateral-to-apical permeability, the preincubation buffer in the apical (receiver) compartment was replaced with 0.5 ml of fresh buffer of desired pH (4.5–8.5) and each Transwell was transferred into a new well containing 1.5 ml of ^{3}H-atazanavir (1 μM) and ^{14}C-D-mannitol (1 μM) radioactive solution of pH 7.4 in the basolateral (donor) compartment. To maintain sink conditions, every 15 min (at t=15 min, 30 min, 45 min, and 60 min) the apical solution from each Transwell was removed into a scintillation vial (for liquid scintillation counting) and replaced with 0.5 ml of fresh apical buffer of the same pH (4.5–8.5). To examine the effect of fasted and fed state on atazanavir permeability, fasted- and fed-state SIF was used in the apical (donor) compartment while pH 7.4 buffer was used in the basolateral (receiver) compartment and the apical-to-basolateral permeability was measured as described above. For experiments examining atazanavir permeability in the presence of inhibitor (PSC833) or acid-reducing drug (omeprazole or cimetidine), inhibitor or drug was added to both compartments (apical and basolateral) during the 20-min preincubation period and 60-min transport period while the flux of atazanavir and D-mannitol was measured. Cumulative flux of ^{3}H-atazanavir and ^{14}C-D-mannitol in apical-to-basolateral or basolateral-to-apical direction was determined in each well over 0–60 min time period to estimate the apparent permeability coefficients (P_{app}) (Eq. 2). Wells were included in the analysis only if P_{app} of mannitol was less than 1×10^{-6} cm/s. Atazanavir efflux ratios at different pH or in the presence of acid-reducing agents were determined according to Eq. 3 using the corresponding P_{app} coefficients for basolateral-to-apical and apical-to-basolateral permeability. Efflux ratios demonstrate the contribution of active transport in restricting (ER > 1) or facilitating (ER < 1) absorptive permeability of the drug.

In Situ Single-Pass Perfusion of Rat Intestine

Open-loop *in situ* single-pass perfusion studies in rat were carried out in accordance with the study protocol approved by the University of Toronto Animal Ethics Committee as described previously (13), with some modifications. Male Sprague–Dawley rats, 300–350 g, obtained from Charles River Laboratories (Wilmington, MA), were housed and handled according to the University of Toronto, Department of Comparative Medicine guidelines and were allowed to acclimatize for 7 days prior to experiments. Before surgery, animals were anaesthetized with isoflurane inhalant anaesthetic and maintained at 37°C throughout surgery and perfusion procedures. The abdominal cavity was opened by midline incision (3–4 cm) and proximal jejunum segment (6–8 cm in length, starting 2 cm after the ligament of Treitz) and distal ileum segment (6–8 cm in length, ending 1 cm before the cecum) were exposed. Each segment was partially opened at each end, rinsed with warmed saline, and ligated at both ends to glass cannulas (inner diameter = 4 mm), which were secured in place with silk sutures. Exposed intestinal segments were placed back into the abdominal cavity and covered with saline-wetted gauze and parafilm. Glass cannulas were then connected to inlet (proximal opening) or outlet (distal opening) tubing. Each segment was perfused at a constant flow rate of 0.2 ml/min using a syringe infusion pump (Harvard Apparatus syringe pump, Model 22) with perfusion buffer containing ^{3}H-atazanavir (10 μM) and ^{14}C-D-mannitol (10 μM), used as marker of paracellular permeability. After atazanavir permeability reached steady state (approximately after 30 min), perfusate exiting from each segment *via* outlet tubing was collected into vials at 10 min intervals. In order to model gradual change in pH which occurs during food intake or following co-administration of acidic/basic drugs or acid-reducing agents, buffer pH was gradually increased from 4.5 to 8.5 (alkalinization) or gradually decreased from 8.5 to 4.5 (acidification). Buffer pH was changed at 40-min intervals to determine the effective permeability of atazanavir and D-mannitol at each pH. The first perfusion period was extended by 30 min to allow atazanavir intestinal permeability to reach steady state prior to determining effective permeability coefficients. To change the perfusion buffer pH, approximately 5 ml of perfusion buffer was used to replace the previous buffer from the segment, followed by perfusion at constant flow rate of 0.2 ml/min. For studies examining the effect of fasted- and fed-state SIF on atazanavir *in situ* intestinal permeability, jejunum and ileum segments in each animal were first perfused with the fasted-state buffer (30 min preincubation and 0–60 min perfusion) and then with the fed-state buffer (60–120 min perfusion), both of which contained ^{3}H-atazanavir (10 μM) and ^{14}C-D-mannitol (10 μM). For studies examining the effect of omeprazole on atazanavir permeability in the jejunum and ileum, steady-state P_{eff} of ^{3}H-atazanavir (10 μM) was assessed at pH 6.5, first in the absence of omeprazole (0–60 min, control) and then in the presence of omeprazole at 10 μM (60–100 min), 50 μM (100–140 min), or 200 μM (140–180 min) concentrations. In a separate set of animals, the pH of the perfusate exiting the segment was evaluated using VWR SympHony pH Meter, model SB70P (VWR International, Mississauga, Ontario). For all pH buffers (4.5–8.5) used in sequence, in the absence or presence of 200 μM omeprazole, the pH measured in the perfusate exiting each segment was within 0.3 log units of the pH value of the corresponding inflow buffer, suggesting that the desired pH within each segment was maintained throughout the perfusion period (data not shown). All collected perfusate samples were weighed in order to determine the change in weight between perfusion buffer entering and exiting each segment. Atazanavir and D-mannitol concentrations in perfusate were measured by ^{3}H and ^{14}C radioactivity counting, respectively. These concentrations were corrected for water reabsorption by gravitational method (using the ratio of inflow/outflow weight). The corrected outlet concentrations of atazanavir and D-mannitol were then used to determine the effective permeability coefficients (P_{eff}) in each intestinal segment at steady state according to Eq. 4.

Data Analysis

For *in vitro* studies evaluating concentration-dependent effect of omeprazole or cimetidine on atazanavir accumulation, the IC_{50} concentrations corresponding to half-maximum inhibitory effect were determined by fitting the data to a sigmoidal dose–response equation (Eq. 1) (21):

$$V_i = \frac{V_c}{1 + ([I]/IC_{50})^n} \quad (1)$$

where V_c and V_i represent atazanavir uptake rate in the absence (control) or presence of inhibitor, respectively; [I] is the inhibitor concentration; and *n* is the Hill coefficient (the largest absolute value for the slope of the curve). Data fitting into the sigmoidal equation was performed by nonlinear least-squares analysis using GraphPad Prism® version 5.01 software.

To determine atazanavir permeability across the Caco-2 cell monolayers grown on Transwell membrane inserts, the data for time-dependent atazanavir flux in the apical-to-basolateral or basolateral-to-apical direction was fitted into Eq. 2 (20):

$$P_{app} = \frac{\Delta Q}{\Delta t} \times \frac{1}{A \times C_o} \quad (2)$$

where P_{app} is the apparent permeability coefficient (cm/s); $\Delta Q/\Delta t$ is the rate of solute flux (mol/s) from donor into the receiver compartment at steady state; A is the surface area of the filter insert (cm^2) and C_o is the initial solute concentration (mol/cm^3) in the donor compartment.

To evaluate the role of active transport in atazanavir directional permeability, the efflux ratio, defined as the quotient of the secretory permeability and the absorptive permeability, was determined according to Eq. 3 (20):

$$ER = \frac{P_{app\,(B-A)}}{P_{app\,(A-B)}} \tag{3}$$

where ER is the efflux ratio; $P_{app\ (B-A)}$ is the apparent permeability coefficient determined across Caco-2 cell monolayers in the basolateral-to-apical direction; $P_{app\ (A-B)}$ is the apparent permeability coefficient determined across Caco-2 monolayers in the apical-to-basolateral direction.

When evaluating atazanavir and D-mannitol intestinal permeability by *in situ* single-pass perfusion of rat intestine, atazanavir and D-mannitol concentrations in the perfusate exiting each segment were corrected for water reabsorption according to the gravitational method, *i.e.*, determining the change in weight between perfusion buffer entering and exiting each segment and adjusting solute concentrations measured in the perfusate accordingly. The corrected outflow concentrations of atazanavir and D-mannitol were then used to determine the effective permeability coefficients in each intestinal segment at steady state (P_{eff}) according to Eq. 4 (22):

$$P_{eff} = \frac{-Q \times ln(C_{out}/C_{in})}{2\pi RL} \tag{4}$$

where P_{eff} is the effective steady-state permeability coefficient (cm/s); Q is the flow rate (0.2 ml/min, converted to cm^3/s); C_{out}/C_{in} is the ratio of the outlet atazanavir or D-mannitol concentration (corrected for water reabsorption) and the corresponding inlet atazanavir or D-mannitol concentration (10 μM); R is the radius of the intestinal segment (0.18 cm); and L is the length of the intestinal segment measured after completion of perfusion (approximately 6–8 cm).

Statistical Analysis

Each *in vitro* (Caco-2 cell) experiment was repeated at least three times using cells from different passages. In an individual experiment, each point represents triplicate trials. All the *in situ* experiments were performed in 4–6 animals and all steady-state permeability coefficients were calculated based on at least 3 separate concentration measurements for the corresponding perfusion interval. Results are presented as mean ± S.E.M. Statistical analysis was performed using GraphPad Prism®, version 5.01 for Microsoft Windows, Graph Pad Software (San Diego, CA, U.S.A.). Statistical significance was assessed by applying the two-tailed Student's *t*-test for unpaired or paired experimental values, or the one-way analysis of variance (ANOVA), the repeated-measures ANOVA, as appropriate. A p value <0.05 was considered statistically significant.

RESULTS

Effect of pH on Atazanavir Accumulation by Caco-2 Cells

In order to examine the effect of pH on atazanavir ability to permeate into the intestinal cells, time-dependent accumulation of 1 μM ^{3}H-atazanavir by Caco-2 cell monolayers was evaluated in buffers of varying pH ranging from 4.5 to 8.5 (Fig. 1a). Initial uptake of atazanavir by Caco-2 cells was independent of buffer pH, since uptake velocities (V_o), estimated from the linear slope (0–1 min) of each time curve, were similar across the range of pH 4.5–8.5 (data not shown). However, net accumulation of atazanavir was sensitive to extracellular pH, with significant differences in accumulation observed after 3 min incubation ($p<0.05$) and up to 30 min incubation ($p<0.001$). Increasing buffer pH resulted in a decreased atazanavir accumulation, although similar accumulation was observed at pH 7.4 and 8.5 (Fig. 1a). Atazanavir accumulation at acidic pH 4.5 was 2.2-fold higher compared to neutral pH 7.4 ($p<0.001$). Since pH appeared to alter atazanavir net accumulation and not the initial uptake velocity, the observed increase in atazanavir net accumulation may be due to a decrease in its efflux by Pgp, the main transporter mediating atazanavir efflux from Caco-2 cells (13). For this purpose we examined the accumulation of 1 μM ^{3}H-atazanavir by Caco-2 cell monolayers at pH 5.5 or 7.4 after 30 min incubation in the absence or presence of Pgp inhibitor, 1 μM PSC833 (Fig. 1b). At pH 5.5, 1uM PSC833 had lower inhibitory effect on atazanavir efflux (78% increase in accumulation, $p<0.001$) compared to pH 7.4 (245% increase in accumulation, $p<0.001$). Furthermore, similar accumulation was observed at pH 5.5 and pH 7.4 ($p=0.81$) when Pgp was inhibited, confirming that the pH sensitivity of atazanavir accumulation may be related to differences in Pgp mediated efflux.

Effect of pH on Atazanavir Lipophilicity

To investigate the role of pH in atazanavir interactions with Pgp, we examined whether pH can affect the ability of atazanavir to interact with cellular lipid bilayer, since Pgp is suggested to bind its substrates from within the bilayer. We

proposed that the extent to which atazanavir partitions into the lipid bilayer might in turn influence the amount of atazanavir available for efflux by Pgp, thereby affecting its ability to accumulate within the cell. To determine the lipid phase partitioning of atazanavir from aqueous solution, atazanavir was dissolved in aqueous solution of varied pH (1–8.5) and its partitioning into organic solvent was determined using 1-octanol, which allows hydrogen bonding (Fig. 2a), or cyclohexane, which does not permit hydrogen bonding (Fig. 2b). Atazanavir partitioned poorly into cyclohexane across a range of pH (negative log D values), with only 2–3% of total atazanavir entering from aqueous solvent into the organic layer at pH 3 or below. With increase in pH, higher fraction of atazanavir was able to enter into cyclohexane layer, gradually increasing to 16% at pH 7.4. The strongest change was observed between pH 4 and 5, near the pKa of atazanavir basic group (4.4), suggesting that atazanavir protonation state and change in charge (from positive to neutral) can strongly influence its ability to partition into cyclohexane. As the pH of the aqueous buffer was decreased from 8.5 to 1, the apparent log D values of atazanavir determined in the cyclohexane:buffer mixture decreased from −0.75 to −1 (Fig. 2a). In contrast, when 1-octanol was used as the organic solvent, atazanavir partitioned very well from the aqueous solution into 1-octanol with more than 96% of total atazanavir entering the organic layer at pH 3 or above. The apparent log D values of atazanavir determined in the 1-octanol:water mixture decreased from 1.78 to 0.65 when buffer pH was decreased from 8.5 to 1 (Fig. 2b).

Effect of pH on Atazanavir Caco-2 Cell Monolayer Permeability

To further assess whether pH affects atazanavir permeability across intestinal epithelium, we examined atazanavir transepithelial flux across Caco-2 cell monolayers grown on polycarbonate Transwell membrane inserts while varying the pH of the luminal (apical compartment) buffer and keeping basolateral buffer pH at 7.4. Atazanavir absorptive permeability, estimated by the apical-to-basolateral P_{app} coefficients (Fig. 3a), was sensitive to changes in luminal pH ($p<0.01$). When pH was gradually increased from acidic (pH 4.5) to neutral (pH 7.4), atazanavir apical-to-basolateral P_{app} gradually decreased from $2.5\pm0.3\times10^{-6}$ cm/s to $1.4\pm0.1\times10^{-6}$ cm/s ($p<0.05$). To evaluate the effect of luminal pH on atazanavir secretory permeability ($P_{app\ (B-A)}$), 1 μM ^{3}H-atazanavir was introduced into the basolateral compartment buffered at pH 7.4 and its appearance in the apical compartment containing buffers of pH 4.5 to 8.5 was measured over time (Fig. 3b). In contrast to absorptive permeability, atazanavir basolateral-to-apical P_{app} was not sensitive to changes in pH of the luminal buffer. Increase in pH was associated with a proportional increase ($R^2=0.95$, $p<0.01$) in atazanavir efflux ratio ($P_{app\ (B-A)}/P_{app\ (A-B)}$), which increased from 5.8 to 11 as apical buffer pH was increased from acidic pH 4.5 to neutral pH 7.4 (data not shown).

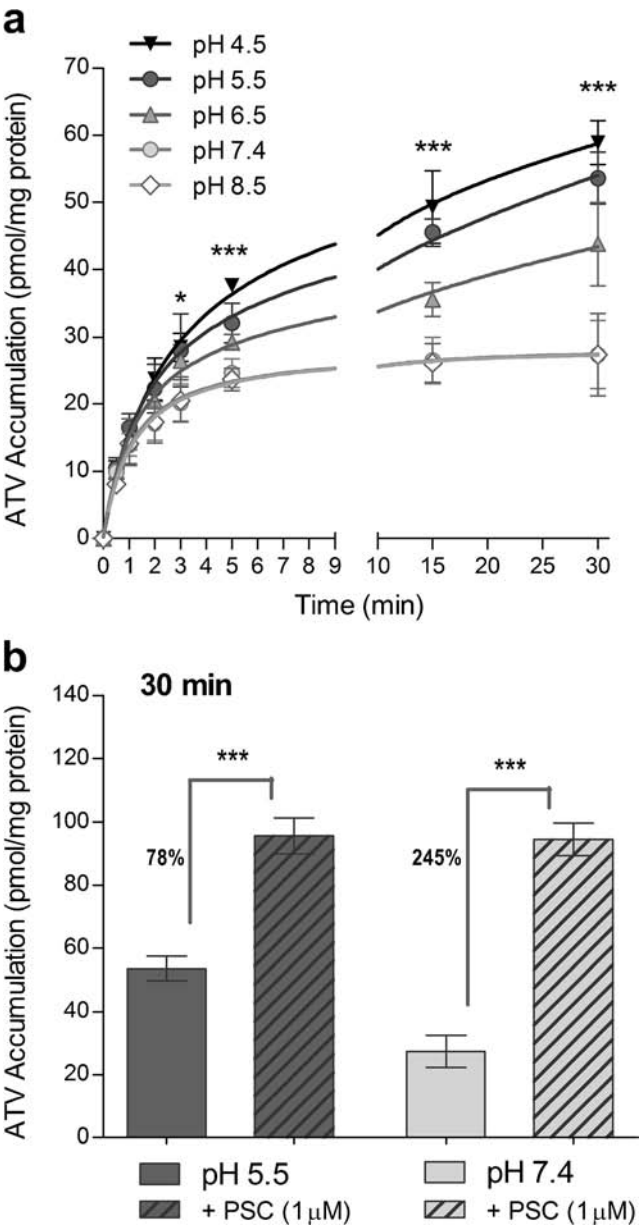

Fig. 1 Effect of pH and Pgp inhibition on atazanavir accumulation by Caco-2 cells. Cellular accumulation of ^{3}H-atazanavir (ATV, 1 μM) by Caco-2 cells was determined at the specified time intervals (0–30 min) in buffers of different pH (4.5–8.5) (**a**). Net accumulation of ^{3}H-atazanavir (1 μM) by Caco-2 cells after 30 min incubation was assessed at pH 5.5 or 7.4 in the absence (control) or presence of 1 μM PSC833 (PSC), an inhibitor of Pgp (**b**). Data represent mean ± S.E.M. of $n=3$ independent experiments. *$p<0.05$; ***$p<0.001$.

Effect of pH on Atazanavir *In Situ* Intestinal Permeability

To confirm the effect of pH on atazanavir intestinal permeability, the steady-state intestinal permeability of atazanavir

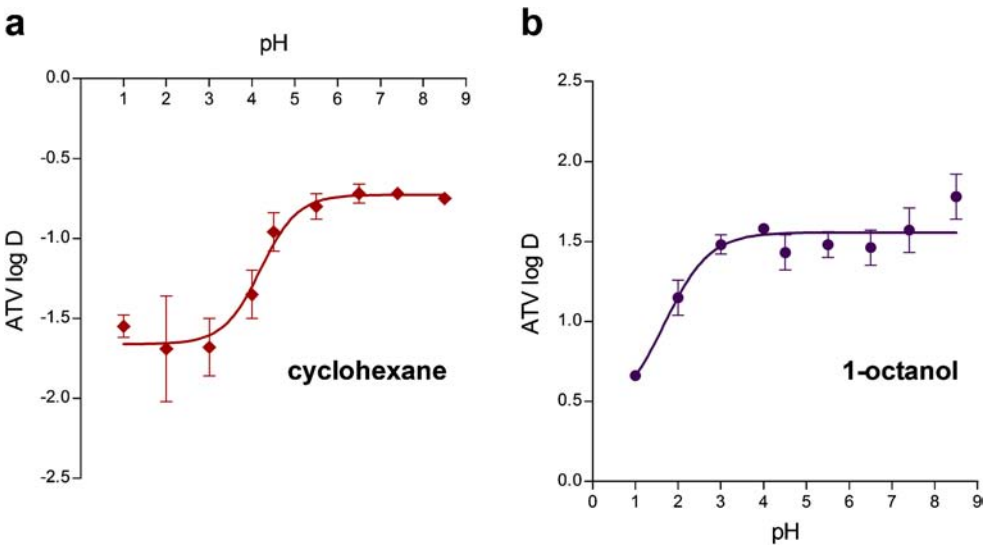

Fig. 2 Effect of pH on atazanavir lipophilicity. Aqueous solutions of different pH (1–8.5) containing 10 μM ^{3}H-atazanavir (ATV) were combined in 1:1 ratio with organic solvent, cyclohexane (**a**) or 1-octanol (**b**). The apparent log D coefficients, determined as log ($C_{organic}/C_{aqueous}$), were calculated in each solvent and plotted as a function of pH of the solution. Data represent mean ± S.E.M. of $n=3$ independent experiments.

(P_{eff}) was evaluated at various luminal pH values by *in situ* single-pass perfusion of rat intestinal segments (Fig. 4). Jejunum and ileum segments in each animal were perfused at 0.2 ml/min flow rate with 10 μM ^{3}H-atazanavir solution at varying buffer pH (4.5–8.5) over a 3.5-h period. To avoid time-dependent bias, three animals were perfused initially with pH 4.5 buffer, followed by pH 5.5, 6.5, 7.4, and finally 8.5 buffer (solid circles, Rat 1, 3, 5). The second set of animals was perfused initially with pH 8.5 buffer followed by pH 7.4, 6.5, 5.5 and finally 4.5 buffer (open circles, Rat 2, 4, 6). Atazanavir concentrations in the perfusate exiting from each segment, corrected for water reabsorption, were used to determine the steady-state P_{eff} of atazanavir at different buffer pH (Fig. 4). Atazanavir steady-state permeability was highly sensitive to changes in intestinal lumen pH. Combined data from six animals demonstrated that a gradual increase in luminal pH from acidic (pH 4.5) to basic pH 8.5 is associated with a gradual decrease in steady-state P_{eff} measured across rat jejunum (2.7-fold, $p<0.001$) and ileum (2.3-fold, $p<0.001$). Furthermore, this effect was independent of the experimental design, *i.e.*, increasing pH from 4.5 to 8.5 *versus* decreasing pH from 8.5 to 4.5, or the intestinal segment examined, with similar effect observed in jejunum and ileum.

Effect of Acid-Reducing Agents on Atazanavir Accumulation by Caco-2 Cells

In order to identify potential pharmacokinetic interactions of PPIs and H_2RAs with atazanavir transport, which are independent of their effect on the gastrointestinal pH, all *in vitro* drug-drug interaction experiments were performed at constant pH and were evaluated at both neutral pH 7.4 and acidic pH 5.5. Because the findings at neutral and acidic pH were similar, only pH 7.4 data are presented in this manuscript. The concentrations of acid-reducing agents used in the interaction studies were selected based on the estimated intestinal concentrations of these drugs during intestinal absorption. Although plasma concentrations of acid-reducing agents are in the low micromolar range (10,23), much higher concentrations are predicted in the intestinal lumen, if oral dose of the drug is completely dissolved in 250 ml volume of gastric fluid (12,22). Based on the estimated intestinal concentrations of omeprazole (116–463 μM for 10–40 mg dose), esomeprazole (107–214 μM for 20–40 mg dose), lansoprazole (162–325 μM for 15–30 mg dose), pantoprazole (197–395 μM for 20–40 mg dose), and rabeprazole (210 μM for 20 mg dose), 200 μM concentrations of these PPIs were used in the initial screening. For H_2RAs, the concentrations estimated in the intestinal fluid varied between different agents: concentrations of famotidine (237–474 μM for 20–40 mg dose) were lower than other drugs in this class (cimetidine, ranitidine, and nizatidine were estimated to reach >1 M concentrations in the intestinal fluid). Hence, 500 μM concentrations of H_2RAs were used in the initial screening (Table I). Net accumulation of 1 μM ^{3}H-atazanavir by Caco-2 cells, after 60 min incubation in the absence (control) or presence of each drug, was increased in the presence of PPIs, omeprazole (36%, $p<0.01$), esomeprazole (31%, $p<0.01$), rabeprazole (38%, $p<0.001$), and lansoprazole (14%, $p<0.05$), but not pantoprazole. In contrast, H_2RAs, cimetidine, nizatidine, famotidine, and ranitidine, did not interfere with atazanavir accumulation by Caco-2 cells.

Omeprazole and Cimetidine Interactions with Atazanavir *In Vitro* Transport and Permeability

For a detailed investigation of potential pharmacokinetic drug-drug interactions between atazanavir and acid-reducing agents, one drug from each mechanistic class, omeprazole (PPI) and cimetidine (H_2RA), was selected for further

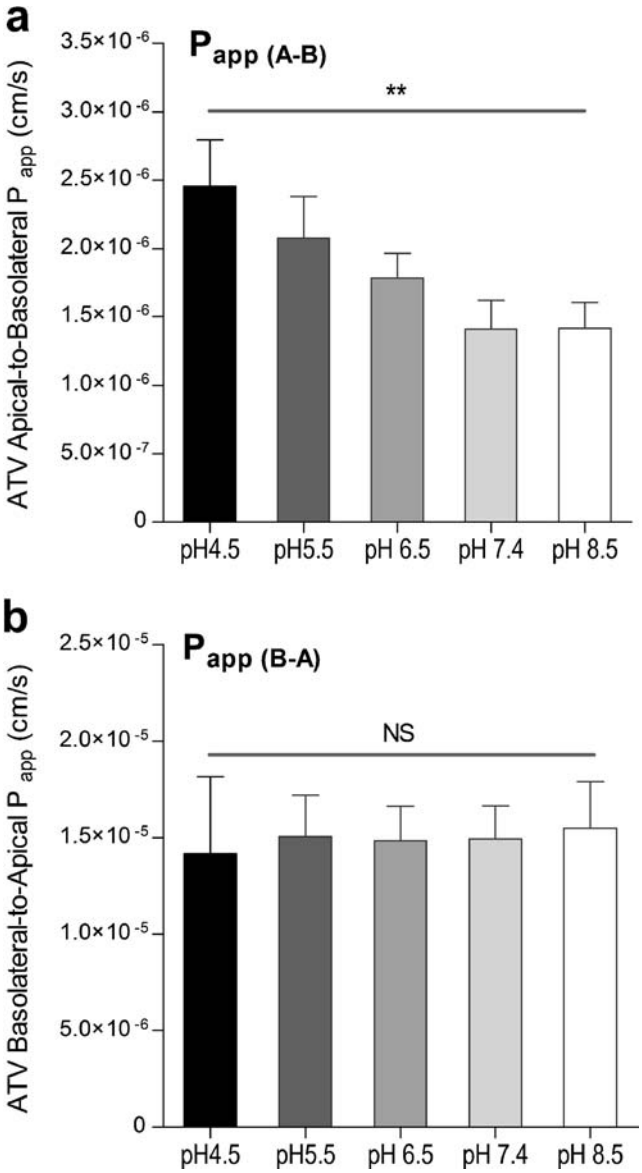

Fig. 3 pH- Dependence of atazanavir *in vitro* intestinal permeability. Atazanavir (ATV) absorptive ($P_{app\ (A-B)}$) (**a**) and secretory ($P_{app\ (B-A)}$) (**b**) permeability coefficients were determined across Caco-2 cell monolayers grown on Transwell membrane inserts at different apical buffer pH (4.5–8.5), while basolateral buffer pH was maintained at 7.4, as described in Materials and Methods. Data represent mean ± S.E.M. of $n = 3$ independent experiments. NS: not significant; $^{**}p < 0.01$.

in vitro studies in Caco-2 cells (Fig. 5). In the presence of 200 μM omeprazole, initial rate of atazanavir uptake by Caco-2 cells was increased 1.9-fold ($p < 0.01$) compared to the DMSO control, but was unchanged in the presence of 500 μM cimetidine (Fig. 5a). The concentration-dependent effect of omeprazole and cimetidine on atazanavir accumulation by Caco-2 cells was measured after 60 min incubation in the absence (control) or presence of increasing concentrations (0.01 – 500 μM) of omeprazole (diamonds) or cimetidine (triangles) (Fig. 5b). Cimetidine did not affect atazanavir accumulation at the range of concentrations tested. In contrast, omeprazole demonstrated a concentration-dependent inhibitory effect on atazanavir efflux, increasing its accumulation at concentrations above 1 μM, with IC_{50} value of 62 μM. Since atazanavir efflux in Caco-2 cells is primarily mediated by Pgp (13), the effect of omeprazole on atazanavir accumulation was examined in the absence or presence of a potent Pgp inhibitor, PSC833 (Fig. 5c). Inhibitory effect of 200 μM omeprazole on atazanavir efflux was less potent compared to 1 μM PSC833 (1.4-fold *versus* 3.1-fold increase in accumulation, respectively). Moreover, when used in combination, omeprazole (200 μM) and PSC833 (1 μM) increased atazanavir accumulation 2.5 fold, a significantly lower inhibitory effect compared to 1 μM PSC833 alone ($p < 0.05$), suggesting that omeprazole may also inhibit atazanavir uptake by Caco-2 cells. When Pgp-mediated efflux was blocked by PSC833, omeprazole inhibited cellular uptake of atazanavir (*i.e.*, decreased atazanavir accumulation) in a concentration-dependent manner with IC_{50} concentration of 170 μM (Fig. 5d). To examine the effect of omeprazole and cimetidine on atazanavir permeability across Caco-2 cell monolayers grown on Transwell membrane inserts, 200 μM omeprazole or 500 μM cimetidine was added to the apical and basolateral compartment buffers during 20-min preincubation period and 60-min atazanavir permeability assay (Fig. 5e). When compared to DMSO control, presence of 200 μM omeprazole resulted in 3.6-fold increase in atazanavir apical-to-basolateral P_{app} ($p < 0.01$) and 45% decrease in its basolateral-to-apical P_{app} ($p < 0.01$), leading to reduction in atazanavir efflux ratio from 11 to 1.6, consistent with the inhibition of Pgp-mediated efflux at the apical membrane of Caco-2 cells. In contrast, cimetidine did not alter atazanavir permeability in the apical-to-basolateral or basolateral-to-apical direction.

Effect of Omeprazole on Atazanavir *In Situ* Intestinal Permeability

In situ single-pass intestinal perfusion model was used to further evaluate the effect of PPI, omeprazole, on the steady-state intestinal permeability of atazanavir in the Sprague–Dawley rat model. Proximal jejunum (Fig. 6a) and distal ileum (Fig. 6b) segments in each animal were perfused with 10 μM ^{3}H-atazanavir buffer (at pH 6.5) in the absence (control; 0–60 min interval) or presence of omeprazole at 10 μM (60–100 min), 50 μM (100–140 min), or 200 μM (140–180 min) concentrations. Atazanavir concentrations in the perfusate exiting each segment, corrected for water reabsorption, were used to determine atazanavir steady-state P_{eff} coefficient for each perfusion period (control, 10 μM, 50 μM, or 200 μM omeprazole). Repeated-measures analysis of variance demonstrated a lack of significant effect of omeprazole on atazanavir steady-state permeability. Furthermore, paired student *t* test comparing P_{eff} values obtained for control *versus* 10 μM, 50 μM, or 200 μM omeprazole separately did not

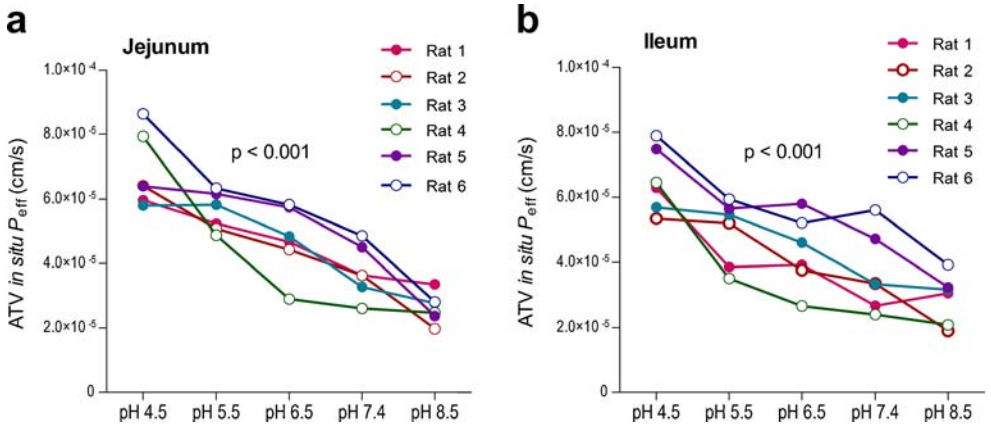

Fig. 4 Effect of pH on atazanavir *in situ* permeability. Atazanavir (ATV) permeability across proximal jejunum (**a**) and distal ileum (**b**) segments was measured in Sprague–Dawley rats. Each segment was perfused at a constant flow rate of 0.2 ml/min with perfusion buffer containing ^{3}H-atazanavir (10 μM) and ^{14}C-D-mannitol (10 μM), used as a marker of paracellular permeability. The pH of the perfusion buffer was changed every 40 min, gradually increasing from pH 4.5 to 8.5 (*solid circles*) or decreasing from pH 8.5 to pH 4.5 (*open circles*). Atazanavir steady-state permeability (P_{eff}) coefficients were determined at each pH (4.5–8.5) and compared within each animal by repeated-measures ANOVA.

reach statistical significance for any omeprazole concentration.

Effect of Fasted and Fed State on Atazanavir Intestinal Permeability

Food intake is known to trigger the release of gastric acid, which lowers gastric pH, consequently leading to a decrease in intestinal lumen pH from 6.5 in fed state to 5.0 in fasted state. In addition, food intake is associated with the release of bile salts (*e.g.*, taurocholate) and phospholipids (*e.g.*, lecithin) in the intestinal tract, which can facilitate drug dissolution and improve solubility. Since atazanavir bioavailability is reported to be influenced by food intake, we proposed that the change in intestinal pH and/or increase in the secretion of bile under fed-state conditions can increase atazanavir intestinal permeability. In agreement with this hypothesis, fed-state buffer (pH 5.0, 15 mM taurocholate, 3.75 mM lecithin) dramatically increased atazanavir absorptive permeability across Caco-2 cell monolayers compared to the fasted-state buffer (pH 6.5, five-fold lower concentrations of taurocholate and lecithin) (Fig. 7a). This effect was much higher than the expected change due to a decrease in pH from 6.5 to 5.0. To further test whether this effect is mediated in part by the increase in concentrations of bile components (*i.e.*, taurocholate and lecithin), "blank" fed- and fasted-state buffers (lacking taurocholate and lecithin) were also tested (Fig. 7b). In the absence of taurocholate and lecithin, the fed-state buffer only moderately increased atazanavir apical-to-basolateral permeability (approximately 2-fold increase, not significant) compared to the fasted-state buffer. Hence, the enhancement in atazanavir *in vitro* permeability under fed-state conditions appears to be largely mediated by the increase in the concentrations of bile components. *In situ* intestinal permeability of atazanavir across rat jejunum (Fig. 7c) and ileum (Fig. 7d) was also significantly higher in fed-state buffer when compared to fasted-state buffer, confirming that fed-state conditions stimulate intestinal permeability of atazanavir.

Table I Effect of Acid-Reducing Agents (PPIs and H_2RAs) on Atazanavir Accumulation by Caco-2 Cell Monolayers

Inhibitor drug	Inhibitor drug concentration	Atazanavir accumulation (% Control)
Control		100 ± 4.4
Proton Pump Inhibitors (PPIs)		
Omeprazole	200 μM	136 ± 10**
Esomeprazole	200 μM	131 ± 9**
Rabeprazole	200 μM	138 ± 4***
Pantoprazole	200 μM	99 ± 4
Lansoprazole	200 μM	114 ± 7*
Histamine$_2$-Receptor Antagonists (H_2RAs)		
Cimetidine	500 μM	94 ± 6
Famotidine	500 μM	93 ± 11
Ranitidine	500 μM	92 ± 4
Nizatidine	500 μM	98 ± 9

*$p < 0.05$, **$p < 0.01$, ***$p < 0.001$

DISCUSSION

The goal of this study was to investigate several mechanisms potentially implicated in atazanavir intestinal absorption and clinical drug-drug interactions with acid-reducing agents. Atazanavir is reported to have pH-dependent aqueous solubility (2) and clinically significant drug-drug interactions with many acid-reducing agents and especially PPIs, which irreversibly block the secretion of gastric acid (24). In this study, we investigated the effect of pH on atazanavir intestinal

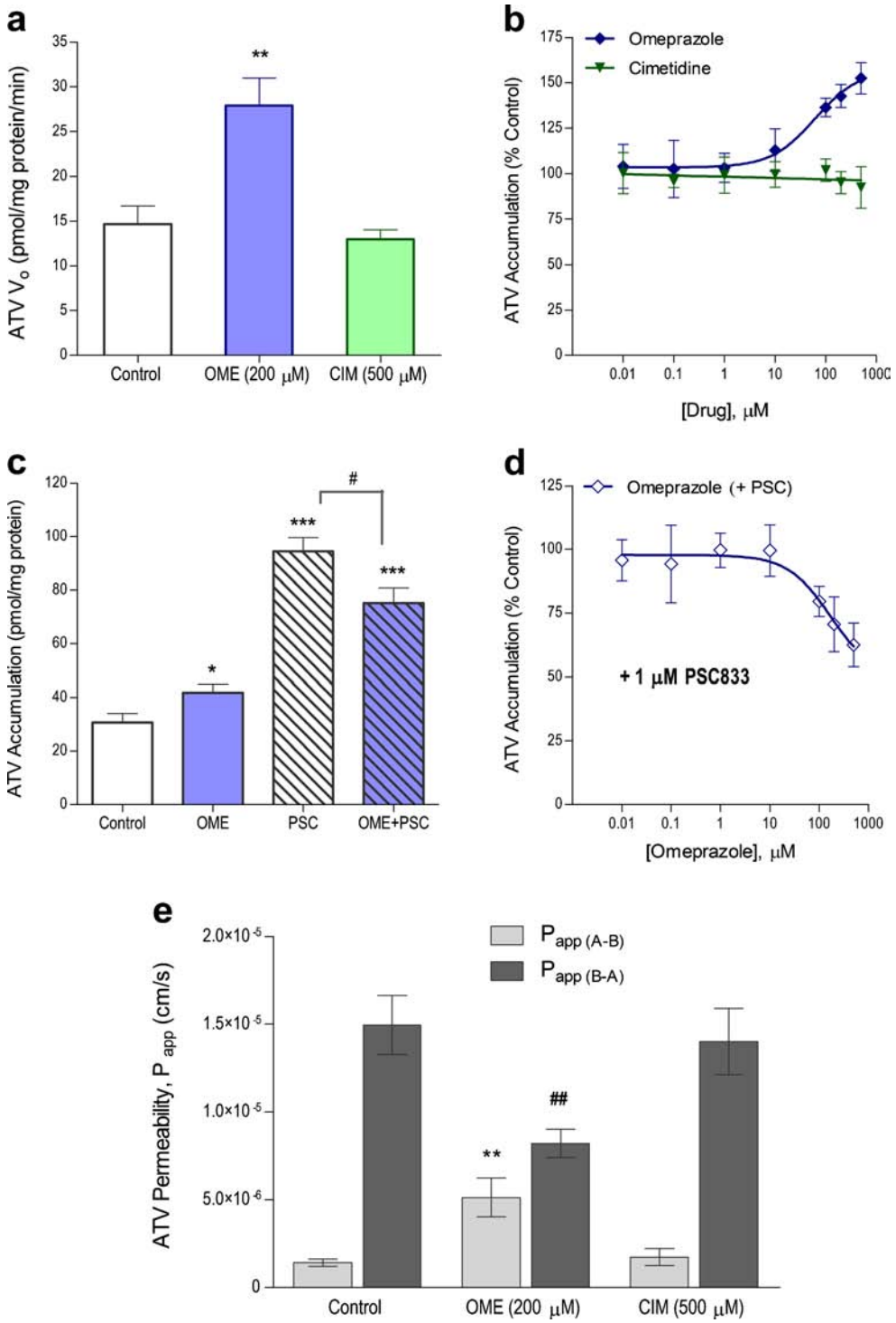

Fig. 5 Interactions of omeprazole and cimetidine with atazanavir transport and permeability in Caco-2 cells. Effect of omeprazole (OME, 200 μM) and cimetidine (CIM, 500 μM) on the initial rate of atazanavir (ATV, 1 μM) uptake by Caco-2 cells was determined at pH 7.4 from the slope of the linear portion (0–1 min) of the time-dependent uptake curve (**a**). Net intracellular accumulation of 1 μM ^{3}H-atazanavir by Caco-2 cells after 30 min incubation was assessed in the absence or presence of increasing concentrations of omeprazole (0.01–500 μM) or cimetidine (0.01–500 μM) (**b**). The effect of omeprazole was also evaluated in the presence of 1 μM PSC833 (PSC), an inhibitor of Pgp, either at constant omeprazole concentration of 200 μM (**c**) or increasing omeprazole concentrations (0.01–500 μM) (**d**). Absorptive ($P_{app\ (A-B)}$) or secretory ($P_{app\ (B-A)}$) permeability of atazanavir was measured in the absence or presence of omeprazole (OME, 200 μM) or cimetidine (CIM, 500 μM) (**e**). Data represent mean ± S.E.M. of $n = 3$ independent experiments. $^{*}p < 0.05$; $^{**}p < 0.01$; $^{***}p < 0.001$; $^{\#}p < 0.05$; $^{\#\#}p < 0.01$.

permeability using Caco-2 cell system, an *in vitro* model of intestinal permeability, and *in situ* single-pass intestinal perfusion.

Atazanavir is a bulky organic base, which can be classified into the BCS class 2 due to its low solubility and high permeability, estimated from the high predicted log *P* values of 4.08–4.54, which is above the log P of metoprolol (1.67) (2,12). Based on this classification, atazanavir is predicted to have high absorption (≥ 90%) (12). However, in this study we report experimental partition coefficients for atazanavir in 1-octanol:buffer mixture that are much lower (log D of 1.43–1.57 for pH 3–7.4) than the predicted log *P* values (4.08–4.54), which are also in agreement with previously reported experimental partition coefficient for atazanavir in 1-octanol:saline

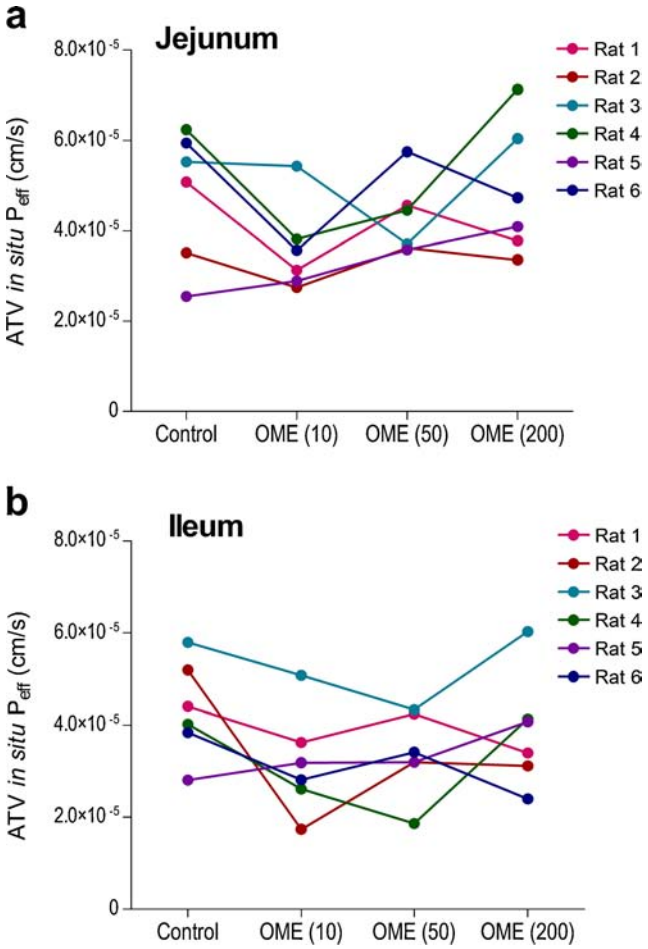

Fig. 6 Effect of omeprazole on atazanavir *in situ* intestinal permeability. *In situ* intestinal permeability (P_{eff}) of atazanavir (ATV) across proximal jejunum (6–8 cm in length, starting 2 cm after the ligament of Treitz) (**a**) and distal ileum (6–8 cm in length, ending 1 cm before the cecum) (**b**) of Sprague–Dawley rats was measured by single-pass intestinal perfusion method in the absence or presence of omeprazole (OME). Each segment was perfused at a constant flow rate of 0.2 ml/min with pH 6.5 perfusion buffer containing ^{3}H-atazanavir (10 μM) and ^{14}C-D-mannitol (10 μM), first in the absence of omeprazole (control, 0–60 min) and then in the presence of omeprazole at 10 μM (60–100 min), 50 μM (100–140 min), or 200 μM (140–180 min) concentrations. The steady-state P_{eff} coefficients were determined in each animal during the four intervals (joined by a line) and compared by repeated measures ANOVA.

mixture (log P of 1.48) (11). Hence, atazanavir may belong to the BCS class 4, which includes drugs with low solubility and low permeability that are predicted to have incomplete absorption (12). Previous studies correlating the permeability of drugs across Caco-2 monolayers with their extent of oral absorption in humans have defined the low/high drug permeability boundary to be between 5.0×10^{-6} and 14.0×10^{-6} cm/s, since model compounds with known low permeability (fraction absorbed<90%) had $P_{app}<5.0\times10^{-6}$ cm/s, while high-permeability compounds (fraction absorbed ≥90%) had P_{app}cm/s (25,26). Hence, based on our *in vitro* Caco-2 permeability data, atazanavir can be classified as a low-permeability compound. Similarly, human extent of absorption has been previously correlated with the *in situ* P_{eff} values determined across rat jejunum at pH 6.5 (26–28). Low permeability model compounds had $P_{eff}<42\times10^{-6}$ cm/s, while high-permeability compounds had $P_{eff}>50.9\times10^{-6}$ cm/s (27). In this study, atazanavir permeability across rat jejunum at pH 6.5 was equal to $47\pm11\times10^{-6}$ cm/s, which falls within the borderline region, highlighting the difficulty in classifying atazanavir as low or high permeability drug. At neutral pH, the P_{eff} decreases to $37\pm12\times10^{-6}$ cm/s and falls in the low permeability range. Given the high variability and pH dependence of the *in situ* atazanavir permeability, as well as the low permeability of atazanavir observed *in vitro* across Caco-2 monolayers, we believe that atazanavir may behave as a low permeability/low solubility compound and hence, should belong to the BCS class 4. Interestingly, intestinal absorption of class 4 drugs is predicted to be influenced by drug uptake and efflux processes (29).

Atazanavir was traditionally believed to enter the cell by simple diffusion. Since its predicted pKa of 4.4 falls in the range of physiological pH observed in the gastrointestinal tract, its absorption can be affected by the equilibrium between the ionized and unionized forms. At acidic pH, atazanavir basic group gains a proton and forms a charged species (organic cation), resulting in improved aqueous solubility (2). However, formation of a charged species may have a negative impact on atazanavir interactions with the lipid bilayer, potentially reducing its membrane permeability during intestinal absorption. Contrary to this prediction, atazanavir accumulation by Caco-2 cells and apical-to-basolateral permeability were increased at acidic pH, when its diffusion across the cell membrane is predicted to be lower. Even after 30 min incubation, when the net accumulation at all pH values reached a steady state, the total amount of atazanavir able to accumulate within the cell was significantly higher under acidic conditions, suggesting potential involvement of a pH-dependent carrier-mediated transport process. Since Caco-2 cells express a variety of drug uptake and efflux transporters and have a negligible expression of CYP3A4 (30), higher steady-state accumulation of atazanavir at acidic pH may be related to increase in uptake, decrease in efflux, or a combination of these mechanisms. Furthermore, the relative contribution of passive diffusion, carrier-mediated uptake, and active efflux could be affected by the pH of the intestinal lumen.

Our group and others have previously demonstrated that atazanavir cellular uptake is in part carrier-mediated and sensitive to inhibition by several OATP family inhibitors (11,13). Hence, higher accumulation of atazanavir at acidic pH may result from increased uptake by this OATP-like transporter. If this uptake carrier preferentially transports the protonated (charged) form of atazanavir abundant at acidic pH, has higher transport activity at acidic pH, or uses an inwardly-directed proton gradient as a driving force, decrease in pH would lead to an increase in atazanavir cellular

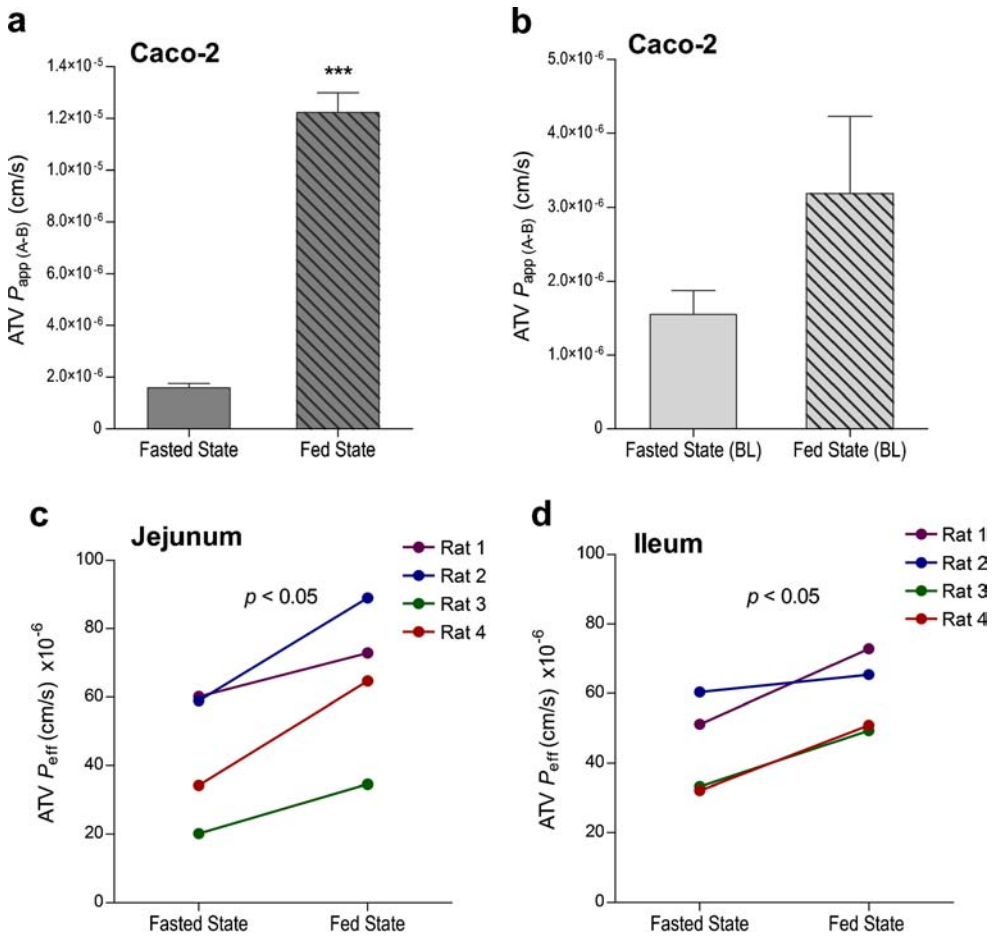

Fig. 7 Influence of fasted- and fed-state conditions on atazanavir intestinal permeability in the *in vitro* and *in situ* models. Absorptive permeability ($P_{app\ (A-B)}$) of 1 μM atazanavir (ATV) across Caco-2 cell monolayers was measured in the presence of fasted- or fed-state simulated intestinal fluid (SIF) buffers (**a**), as described in Materials and Methods, or in the presence of "Blank" fasted- or fed-state SIF buffers, which lacked the components of bile, taurocholate and egg lecithin (**b**). Data represent mean ± S.E.M. for $n = 3$ independent experiments. In Sprague–Dawley rats, steady-state permeability of atazanavir across jejunum (**c**) or ileum (**d**) segments was assessed by perfusing each segment with 10 μM ^{3}H-atazanavir solution dissolved first in the fasted-state SIF buffer (0–60 min) and then in the fed-state SIF buffer (60–120 min), as described in Materials and Methods. The steady-state P_{eff} coefficients determined for fasted- and fed-state SIF buffers in each animal (joined by a line) were compared by paired Student's *t*-test analysis. ***$p < 0.001$.

uptake. However, in our early-time uptake studies we observed similar atazanavir uptake velocities across a range of pH (4.5–8.5), inconsistent with the presence of a pH-dependent carrier-mediated uptake process. When Pgp-mediated transport was inhibited, we observed similar atazanavir accumulation at acidic and neutral pH, suggesting that the carrier-mediated uptake of atazanavir by Caco-2 cells is independent of pH. In addition, in our previous study we have demonstrated that the reversal of the proton gradient by intracellular acidification method did not affect atazanavir uptake or accumulation by Caco-2 cells, further confirming that this uptake transporter is not driven by a proton gradient (21).

The second potential explanation for increased net accumulation of atazanavir at acidic pH is decrease in active efflux. We have previously shown that atazanavir efflux from Caco-2 cells is primarily mediated by Pgp (13). Pgp inhibitors, PSC833 and GF120918, increased atazanavir accumulation by Caco-2 cells (3.5- and 3.3-fold, respectively), increased its apical-to-basolateral permeability (4.5- and 5.6-fold, respectively), and decreased the efflux ratio across Caco-2 monolayers from 11.6 (in the absence of inhibitors) to 1.5 (13). Although atazanavir is also reported to be a substrate of several MRP isoforms (11,15,31), in our previous study we have demonstrated that MRP family inhibitors do not increase atazanavir accumulation by Caco-2 cells, suggesting that MRPs, such as MRP2 transporter highly expressed at the brush-border membrane of enterocytes, have a minor contribution to atazanavir intestinal transport (13). Hence, in this study, we tested the hypothesis that a decrease in pH is associated with lower atazanavir efflux by Pgp at the apical membrane of Caco-2 cells, thereby leading to higher net accumulation and apical-to-basolateral permeability of atazanavir. Our data demonstrated a lower inhibitory effect of 1 μM PSC833 on Pgp-mediated efflux of atazanavir at pH 5.5 (78%) compared to pH 7.4 (245%) and similar net accumulation of atazanavir by Caco-2 cells at pH 5.5 and pH 7.4 when Pgp was inhibited.

Many potential mechanisms could be responsible for the apparent decrease in Pgp-mediated efflux of atazanavir at acidic pH: i) decreased binding of atazanavir to Pgp from within the lipid bilayer due to lower membrane partitioning of atazanavir at acidic pH (32–34), ii) modulation of Pgp functional activity either by extracellular pH or the presence of a pH gradient across the brush-border membrane (35–37), or iii) changes in the relative contribution of passive diffusion, carrier-mediated uptake, and active efflux, which could be related to the protonation state of atazanavir at the different

pH conditions. In this study, we have demonstrated that atazanavir partitioned favourably into 1-octanol (> 96%) across a range of pH (3–8.5) with log D values similar to the octanol:saline partition coefficient (log P of 1.48) reported previously (11). However, atazanavir interactions with a more lipophilic solvent were not favourable and were strongly influenced by changes in pH. Only 2–3% of total atazanavir partitioned into cyclohexane at pH 3 or lower, when atazanavir was primarily positively charged, compared to 16% partitioning at pH 7.4, when atazanavir was primarily unionized (neutral). Atazanavir partitioning into the lipid bilayer (also lipophilic) may be similarly reduced at acidic pH. Further studies are needed to examine the link between these membrane partitioning properties of atazanavir, its intestinal membrane permeability, and Pgp-mediated efflux.

In the *in situ* intestinal perfusion model, atazanavir permeability was also sensitive to changes in luminal pH. Within each animal, gradual alkalinization of the perfusion buffer, which imitates the increase in pH of intestinal lumen following administration of acid-reducing agents, resulted in lower steady-state permeability of atazanavir across rat jejunum and ileum. These findings agree with the clinically reported decrease in atazanavir plasma concentrations when co-administered with acid-reducing agents, which pharmacologically increase gastric and consequently intestinal pH. Atazanavir P_{eff} coefficients determined in jejunum and ileum were similar. Pgp expression has been reported to increase from proximal to distal segments of the rat intestine (38,39). While some studies report higher expression of Pgp in the ileum as compared to jejunum (39), others demonstrate similar Mdr1a gene and Pgp protein expression in these two segments (38). In addition, similar efflux ratios for digoxin across rat jejunum (4.4±1) and ileum (4.2±0.5) were reported by *ex vivo* Ussing chamber method (40). Furthermore, in our previous study examining the role of drug transporters in atazanavir intestinal permeability, we reported similar effect of the Pgp inhibitor, PSC833, on atazanavir *in situ* permeability across rat jejunum and ileum, *i.e.*, 78% and 79% increase in atazanavir P_{eff}, respectively, determined in 10 animals (13). Collectively, these findings suggest that the functional activity of Pgp in rodents may be similar in rat jejunum and ileum.

Clinical drug-drug interactions of atazanavir with acid-reducing agents are likely to be resulting from pharmacological pH changes induced by these drugs, which increase gastric pH above 3 and are also reported as indirectly increase the pH of the intestinal lumen (10). However, since PPIs and H_2RAs are also known to interact with drug transporters, we investigated potential interactions between atazanavir and co-administered PPIs and H_2RAs in the intestine. *In vitro*, all PPIs except pantoprazole moderately increased atazanavir accumulation (14–38%), while no significant interactions were observed between atazanavir and H_2RAs. The increase in atazanavir accumulation by PPIs, and in particular omeprazole, was most likely due to Pgp inhibition. Omeprazole was previously shown to inhibit Pgp-mediated efflux of digoxin, an established Pgp substrate, with an IC_{50} concentration of 17.7 μM and 2.6-fold increase in the apical-to-basolateral permeability of digoxin across Caco-2 cell monolayers (41,42). The effect of omeprazole on atazanavir accumulation was less profound with an IC_{50} concentration of 62 μM. Although *in vitro*, omeprazole inhibited atazanavir efflux and, to a lesser extent, uptake by Caco-2 cells, *in situ* permeability of atazanavir was not significantly altered by omeprazole. These discrepancies between the findings from *in situ* and *in vitro* models could be potentially explained by the species differences in the expression and functional activity of drug transporter such as Pgp and OATPs, as well as the increased complexity of the *in situ* model, which accounts for drug metabolism and mucosal microenvironment at the brush-border membrane, unlike the Caco-2 cell system (27,30). Furthermore, the expression of Pgp is reported to be higher in Caco-2 cells compared to human or rat jejunum (43). Thus, Pgp-mediated interactions may be overestimated in this *in vitro* model. Given that omeprazole only moderately inhibited atazanavir efflux and uptake in Caco-2 cells, these pharmacokinetic interactions are expected to play a minor role *in vivo*, suggesting that the pharmacological effect of omeprazole on gastrointestinal pH is responsible for the observed clinical drug-drug interactions.

Since atazanavir is reported to have improved oral bioavailability under fed-state conditions associated with the release of gastric acid and secretion of bile, we investigated the effect of "food intake" on atazanavir intestinal permeability using previously established buffers simulating intestinal fluid under fasted- and fed-state conditions (19). Under fed-state conditions, atazanavir absorptive permeability was significantly higher and this effect required the presence of bile components (five-fold higher under fed-state conditions), suggesting that atazanavir intestinal permeability is dependent not only on the change in pH but also on the composition of the intestinal fluid. Bile components released after food intake, such as bile salts (*e.g.*, taurocholate) and phospholipids (*e.g.*, lecithin), are known to facilitate the wetting of solids and solubilization of lipophilic drugs into mixed micelles (44). However, in this study atazanavir was fully solubilized in the aqueous buffer at 1 μM (*in vitro*) or 10 μM (*in situ*) concentrations, making further enhancement in atazanavir solubility unlikely. Nonetheless, atazanavir *in vitro* and *in situ* permeability was increased in fed-state buffer, in part due to the presence of five-fold higher concentrations of bile components. Interestingly, some phospholipids are known to act as permeability enhancers (45,46). Presence of these molecules in the intestinal lumen has been associated with destabilization of cell membranes and lipid-induced alterations in intracellular events, which can lead to intestinal cell damage and alteration of tight junctions between the gastrointestinal epithelial cells, thereby changing the integrity of the intestinal membrane (45). Further studies are

needed to elucidate the nature of atazanavir interactions with various bile salts and phospholipids released during food intake.

CONCLUSION

Our *in vitro* and *in situ* data demonstrate for the first time that atazanavir intestinal permeability can be influenced by changes in intestinal pH and the amount of bile salts and phospholipids present during absorption. These findings agree with the clinical studies reporting that atazanavir plasma concentrations are highly sensitive to interactions with drugs that modulate gastric pH and food intake, which triggers the release of gastric acid and the secretion of bile. Considering the complexity of atazanavir oral absorption, it is not surprizing that bioavailability and plasma pharmacokinetics of atazanavir vary greatly between individuals. High variability in atazanavir pharmacokinetics reported clinically could potentially be explained by: i) interindividual differences in gastric pH and bile output; ii) high variability in Pgp and CYP3A4 expression and activity; and iii) the effect of co-administered drugs, diet, and disease state on the gastrointestinal pH and CYP3A4 and Pgp expression and activity. In the context of HIV infection, HIV disease progression and antiretroviral treatment are associated with many gastrointestinal abnormalities which have been reported to alter the acidity of the gastrointestinal fluid causing hypohydrochloria (5). Interestingly, atazanavir C_{max} and AUC are reported to be significantly lower in HIV-infected patients (2). We believe that this observation could be explained by reduced absorption of atazanavir, due to lower solubility and/or lower intestinal permeability of atazanavir as a result of increased gastric and intestinal pH. This could provide a potential strategy for improving atazanavir oral bioavailability by manipulating gastrointestinal pH. In addition, the expression of Pgp and CYP3A4 may differ in HIV-infected patients compared to healthy subjects, since many enzymes and drug transporters are reported to be regulated by antiretroviral drugs and other co-administered medications as well as inflammatory pathways associated with the HIV infection of the gut-associated lymphoid tissue (14,47,48). Further studies are necessary to fully elucidate the effect of HIV infection and its treatment on gastric and intestinal pH, the expression of intestinal drug transporters and metabolic enzymes, and the bioavailability of antiretroviral drugs to further optimize current and future antiretroviral regimens in HIV-infected patients.

ACKNOWLEDGMENTS AND DISCLOSURES

This work is supported by an operating grant from the Canadian Foundation for AIDS Research Grant #20023, awarded to Dr. Reina Bendayan. Drs. Reina Bendayan and Sharon Walmsley are recipients of the Ontario HIV Treatment Network (OHTN) Career Scientist award. Ms. Olena Kis was supported by Ph.D. studentships from the OHTN, Ministry of Health of Ontario, and the Canadian Institutes of Health Research (CIHR) Frederick Banting and Charles Best – Canada Graduate Scholarship.

We thank Dr. David E. Smith, Department of Pharmaceutical Sciences, University of Michigan College of Pharmacy, for excellent guidance with the implementation of the rodent *in situ* single-pass perfusion technique and Dr. Carolyn Cummins, Department of Pharmaceutical Sciences, University of Toronto, for helpful advice in the design of *in vitro* and *in situ* experiments.

REFERENCES

1. Panel on Antiretroviral Guidelines for Adults and Adolescents. Guidelines for the use of antiretroviral agents in HIV-1 infected adults and adolescents. Department of Health and Human Services; 2013 February 12. Available from: http://aidsinfo.nih.gov/ContentFiles/AdultandAdolescentGL.pdf.
2. Bristol-Myers Squibb Company. REYATAZ® (atazanavir sulfate) Capsules: Prescribing Information. Bristol-Myers Squibb Company; 2013 August. Available from: http://packageinserts.bms.com/pi/pi_reyataz.pdf.
3. Bristol-Myers Squibb Company. BMS-232632: Atazanavir briefing document. Bristol-Myers Squibb Company; 2003 May. Available from: http://www.fda.gov/ohrms/dockets/ac/03/briefing/3950B1_01_bristolmyerssquibb-atazanavir.pdf.
4. Busti AJ, Hall RG, Margolis DM. Atazanavir for the treatment of human immunodeficiency virus infection. Pharmacotherapy. 2004;24(12):1732–47.
5. Welage LS, Carver PL, Revankar S, Pierson C, Kauffman CA. Alterations in gastric acidity in patients infected with human immunodeficiency virus. Clin Infect Dis. 1995;21(6):1431–8.
6. Zhu L, Persson A, Mahnke L, Eley T, Li T, Xu X, *et al.* Effect of low-dose omeprazole (20 mg daily) on the pharmacokinetics of multiple-dose atazanavir with ritonavir in healthy subjects. J Clin Pharmacol. 2011;51(3):368–77.
7. Luber AD, Brower R, Kim D, Silverman R, Peloquin CA, Frank I. Steady-state pharmacokinetics of once-daily fosamprenavir/ritonavir and atazanavir/ritonavir alone and in combination with 20 mg omeprazole in healthy volunteers. HIV Med. 2007;8(7):457–64.
8. Agarwala S, Gray K, Wang Y, Grasela D. Pharmacokinetic effect of omeprazole on atazanavir coadminstered with ritonavir in healthy subjects. 12th Conference on Retroviruses and Opportunistic Infections. 2005 February 22.
9. Wang X, Boffito M, Zhang J, Chung E, Zhu L, Wu Y, *et al.* Effects of the H2-receptor antagonist famotidine on the pharmacokinetics of atazanavir-ritonavir with or without tenofovir in HIV-infected patients. AIDS Patient Care STDS. 2011;25(9):509–15.
10. Shin JM, Kim N. Pharmacokinetics and pharmacodynamics of the proton pump inhibitors. J Neurogastroenterol Motil. 2013;19(1):25–35.
11. Janneh O, Anwar T, Jungbauer C, Kopp S, Khoo SH, Back DJ, *et al.* P-glycoprotein, multidrug resistance-associated proteins and human organic anion transporting polypeptide influence the intracellular accumulation of atazanavir. Antivir Ther. 2009;14(7):965–74.

12. Dahan A, Miller JM, Amidon GL. Prediction of solubility and permeability class membership: provisional BCS classification of the world's top oral drugs. AAPS J. 2009;11(4):740–6.
13. Kis O, Zastre JA, Hoque MT, Walmsley SL, Bendayan R. Role of drug efflux and uptake transporters in atazanavir intestinal permeability and drug-drug interactions. Pharm Res. 2013;30(4):1050–64.
14. Kis O, Robillard K, Chan GN, Bendayan R. The complexities of antiretroviral drug-drug interactions: role of ABC and SLC transporters. Trends Pharmacol Sci. 2010;31(1):22–35.
15. Bierman WF, Scheffer GL, Schoonderwoerd A, Jansen G, van Agtmael MA, Danner SA, *et al.* Protease inhibitors atazanavir, lopinavir and ritonavir are potent blockers, but poor substrates, of ABC transporters in a broad panel of ABC transporter-overexpressing cell lines. J Antimicrob Chemother. 2010;65(8):1672–80.
16. Li W, Zeng S, Yu LS, Zhou Q. Pharmacokinetic drug interaction profile of omeprazole with adverse consequences and clinical risk management. Ther Clin Risk Manag. 2013;9:259–71.
17. Ito S, Kusuhara H, Yokochi M, Toyoshima J, Inoue K, Yuasa H, *et al.* Competitive inhibition of the luminal efflux by multidrug and toxin extrusions, but not basolateral uptake by organic cation transporter 2, is the likely mechanism underlying the pharmacokinetic drug-drug interactions caused by cimetidine in the kidney. J Pharmacol Exp Ther. 2012;340(2):393–403.
18. Moss DM, Siccardi M, Murphy M, Piperakis MM, Khoo SH, Back DJ, *et al.* Divalent metals and pH alter raltegravir disposition in vitro. Antimicrob Agents Chemother. 2012;56(6):3020–6.
19. Klein S. The use of biorelevant dissolution media to forecast the in vivo performance of a drug. AAPS J. 2010;12(3):397–406.
20. Hubatsch I, Ragnarsson EG, Artursson P. Determination of drug permeability and prediction of drug absorption in Caco-2 monolayers. Nat Protoc. 2007;2(9):2111–9.
21. Kis O, Zastre JA, Ramaswamy M, Bendayan R. pH dependence of organic anion-transporting polypeptide 2B1 in Caco-2 cells: potential role in antiretroviral drug oral bioavailability and drug-drug interactions. J Pharmacol Exp Ther. 2010;334(3):1009–22.
22. Dahan A, Amidon GL. Segmental dependent transport of low permeability compounds along the small intestine due to P-glycoprotein: the role of efflux transport in the oral absorption of BCS class III drugs. Mol Pharm. 2009;6(1):19–28.
23. Lin JH. Pharmacokinetic and pharmacodynamic properties of histamine H2-receptor antagonists. Relationship between intrinsic potency and effective plasma concentrations. Clin Pharmacokinet. 1991;20(3):218–36.
24. Fulco PP, Vora UB, Bearman GM. Acid suppressive therapy and the effects on protease inhibitors. Ann Pharmacother. 2006;40(11):1974–83.
25. Volpe DA, Faustino PJ, Ciavarella AB, Asafu-Adjaye EB, Ellison CD, Yu LX, *et al.* Classification of drug permeability with a Caco-2 cell monolayer assay. Clin Res Regul Aff. 2007;24(1):39–47.
26. Volpe DA. Application of method suitability for drug permeability classification. AAPS J. 2010;12(4):670–8.
27. Zakeri-Milani P, Valizadeh H, Tajerzadeh H, Islambulchilar Z. The utility of rat jejunal permeability for biopharmaceutics classification system. Drug Dev Ind Pharm. 2009;35(12):1496–502.
28. Kim JS, Mitchell S, Kijek P, Tsume Y, Hilfinger J, Amidon GL. The suitability of an in situ perfusion model for permeability determinations: utility for BCS class I biowaiver requests. Mol Pharm. 2006;3(6):686–94.
29. Benet LZ. Predicting drug disposition via application of a Biopharmaceutics Drug Disposition Classification System. Basic Clin Pharmacol Toxicol. 2010;106(3):162–7.
30. Taipalensuu J, Tornblom H, Lindberg G, Einarsson C, Sjoqvist F, Melhus H, *et al.* Correlation of gene expression of ten drug efflux proteins of the ATP-binding cassette transporter family in normal human jejunum and in human intestinal epithelial Caco-2 cell monolayers. J Pharmacol Exp Ther. 2001;299(1):164–70.
31. Zastre JA, Chan GN, Ronaldson PT, Ramaswamy M, Couraud PO, Romero IA, *et al.* Up-regulation of P-glycoprotein by HIV protease inhibitors in a human brain microvessel endothelial cell line. J Neurosci Res. 2009;87(4):1023–36.
32. Simon S, Roy D, Schindler M. Intracellular pH and the control of multidrug resistance. Proc Natl Acad Sci U S A. 1994;91(3):1128–32.
33. Aller SG, Yu J, Ward A, Weng Y, Chittaboina S, Zhuo R, *et al.* Structure of P-glycoprotein reveals a molecular basis for poly-specific drug binding. Science. 2009;323(5922):1718–22.
34. Clay AT, Sharom FJ. Lipid bilayer properties control membrane partitioning, binding, and transport of p-glycoprotein substrates. Biochemistry. 2013;52(2):343–54.
35. Thews O, Dillenburg W, Fellner M, Buchholz HG, Bausbacher N, Schreckenberger M, *et al.* Activation of P-glycoprotein (Pgp)-mediated drug efflux by extracellular acidosis: in vivo imaging with 68Ga-labelled PET tracer. Eur J Nucl Med Mol Imaging. 2010;37(10):1935–42.
36. Thews O, Dillenburg W, Rosch F, Fellner M. PET imaging of the impact of extracellular pH and MAP kinases on the p-glycoprotein (Pgp) activity. Adv Exp Med Biol. 2013;765:279–86.
37. Lotz C, Kelleher DK, Gassner B, Gekle M, Vaupel P, Thews O. Role of the tumor microenvironment in the activity and expression of the p-glycoprotein in human colon carcinoma cells. Oncol Rep. 2007;17(1):239–44.
38. MacLean C, Moenning U, Reichel A, Fricker G. Closing the gaps: a full scan of the intestinal expression of p-glycoprotein, breast cancer resistance protein, and multidrug resistance-associated protein 2 in male and female rats. Drug Metab Dispos. 2008;36(7):1249–54.
39. Dahan A, Sabit H, Amidon GL. Multiple efflux pumps are involved in the transepithelial transport of colchicine: combined effect of p-glycoprotein and multidrug resistance-associated protein 2 leads to decreased intestinal absorption throughout the entire small intestine. Drug Metab Dispos. 2009;37(10):2028–36.
40. Stephens RH, O'Neill CA, Warhurst A, Carlson GL, Rowland M, Warhurst G. Kinetic profiling of P-glycoprotein-mediated drug efflux in rat and human intestinal epithelia. J Pharmacol Exp Ther. 2001;296(2):584–91.
41. Pauli-Magnus C, Rekersbrink S, Klotz U, Fromm MF. Interaction of omeprazole, lansoprazole and pantoprazole with P-glycoprotein. Naunyn Schmiedebergs Arch Pharmacol. 2001;364(6):551–7.
42. Collett A, Tanianis-Hughes J, Carlson GL, Harwood MD, Warhurst G. Comparison of P-glycoprotein-mediated drug-digoxin interactions in Caco-2 with human and rodent intestine: relevance to in vivo prediction. Eur J Pharm Sci. 2005;26(5):386–93.
43. Hilgendorf C, Ahlin G, Seithel A, Artursson P, Ungell AL, Karlsson J. Expression of thirty-six drug transporter genes in human intestine, liver, kidney, and organotypic cell lines. Drug Metab Dispos. 2007;35(8):1333–40.
44. Carey MC, Small DM. Micelle formation by bile salts. Physical-chemical and thermodynamic considerations. Arch Intern Med. 1972;130(4):506–27.
45. Ilback NG, Nyblom M, Carlfors J, Fagerlund-Aspenstrom B, Tavelin S, Glynn AW. Do surface-active lipids in food increase the intestinal permeability to toxic substances and allergenic agents? Med Hypotheses. 2004;63(4):724–30.
46. Cao X, Yu L, Sun D. Drug absorption principles. In: Krishna R, Yu L, editors. Biopharmaceutics applications in drug development. USA: Springer; 2008. p. 75–100.
47. Urquhart BL, Tirona RG, Kim RB. Nuclear receptors and the regulation of drug-metabolizing enzymes and drug transporters: implications for interindividual variability in response to drugs. J Clin Pharmacol. 2007;47(5):566–78.
48. Koutsounas I, Theocharis S, Patsouris E, Giaginis C. Pregnane X receptor (PXR) at the crossroads of human metabolism and disease. Curr Drug Metab. 2013;14(3):341–50.